PAPER

Throughput Comparison of Turbo-Coded HARQ in OFDM, MC-CDMA and DS-CDMA with Frequency-Domain Equalization

Deepshikha GARG[†a)], ***Student Member and*** **Fumiyuki ADACHI**[†], ***Member***

SUMMARY OFDM, MC-CDMA and DS-CDMA are being researched vigorously as the prospective signaling technique for the next generation mobile communications systems, which will be characterized by the broadband packet technology. With packet transmissions, hybrid ARQ (HARQ) will be inevitable for error control. HARQ with rate compatible punctured turbo (RCPT) codes is one of the promising techniques. Data rate equivalent to the OFDM system can be attained with MC-CDMA and DS-CDMA by assigning all the available codes to the same user resulting in what is commonly referred to as multicode MC-CDMA and multicode DS-CDMA. A rake receiver is used for receiving the DS-CDMA signals. However, recently minimum mean square error frequency-domain equalization (MMSE-FDE) has been proposed for the reception of DS-CDMA signals. In this paper, we introduce RCPT HARQ to DS-CDMA with MMSE-FDE and compare its throughput performance with OFDM, multicode MC-CDMA and multicode DS-CDMA with rake combining. MMSE weight for packet combining is introduced and the soft value generation for turbo coding in MC-CDMA and DS-CDMA with MMSE-FDE is presented. The throughput is theoretically evaluated for the uncoded case. For RCPT-HARQ, the comparison is done by computer simulations. It is found that the throughput of HARQ using DS-CDMA with MMSE-FDE is the same as or better than using MC-CDMA. However, with higher level modulation, type I HARQ using OFDM is better than using either MC-CDMA or DS-CDMA; for type II HARQ without redundancy in the first transmission, however, MC-CDMA and DS-CDMA gives a higher throughput.
key words: *OFDM, multicode MC-CDMA, multicode DS-CDMA, MMSE frequency-domain equalization, RCPT HARQ*

1. Introduction

Broadband wireless packet technology is one of the core technologies for the next generation mobile communications systems. Direct sequence code division multiple access (DS-CDMA) has been adopted as the signaling technique for the third generation mobile communications systems [1] and is a likely candidate for the next generation, as well. Recently, the combination of multicarrier (MC) modulation based on orthogonal frequency division multiplexing (OFDM) [2] and code division multiple access (CDMA), called MC-CDMA [3], [4], has gained a lot of attention because of its ability to allow high data rate transmission in a harsh mobile environment and has emerged as the most promising candidate for the next generation mobile communications systems. Hence, DS-CDMA, OFDM and MC-CDMA are the major contenders for wireless signaling technique. The bit error rate (BER) performances of these signaling techniques have been compared in some recent publications [2]–[4]. In [5], the packet error rate (PER) performance of MC/DS-CDMA (DS-CDMA for multiple subcarriers) is compared with that of MC-CDMA and shown that for downlink, MC-CDMA gives a better performance than MC/DS-CDMA and DS-CDMA; however, in the comparison, rake combining is used for the reception of DS-CDMA signals.

Recently it has been shown that an effective technique to improve the BER performance of DS-CDMA is to apply minimum mean square error frequency-domain equalization (MMSE-FDE) [6]–[8]. It is shown in [6] that DS-CDMA with MMSE-FDE provides a BER performance better than that with rake combining and is comparable to that of MC-CDMA with MMSE-FDE in a frequency selective Rayleigh fading channel. For packet transmissions, the frequency selectivity of the channel is not always desirable. With higher frequency selectivity, the errors are randomized; however, for packet transmissions burst errors are preferable to random errors. Hence, there is a need to evaluate the performance of packet transmissions in a frequency selective channel. For packet transmissions, some form of error control is necessary. To the best of authors' knowledge, the throughput performance of DS-CDMA with MMSE-FDE in the presence of error-control coding has not been evaluated yet. Hybrid ARQ (HARQ) with rate compatible punctured turbo (RCPT) codes [9], [10] is one of the promising error control techniques. In this paper, we introduce RCPT HARQ to DS-CDMA with MMSE-FDE and evaluate the performance improvement over DS-CDMA with rake combining. In addition, the throughput performance of DS-CDMA is compared with OFDM and MC-CDMA. For turbo decoding, soft decision values are needed. They can be generated using the log-likelihood ratio (LLR) [11]. However, the LLR computation for DS-CDMA with FDE is not treated in any paper. In this paper, we show how the LLR is computed for DS-CDMA with MMSE-FDE and show the difference from the LLR for MC-CDMA. In addition, the MMSE weight for packet combining is introduced. When the same packet is transmitted more than once, the MMSE weight needs to be updated with each retransmission to obtain the time diversity gain.

For a fair comparison, we keep the transmission rate

Manuscript received May 6, 2004.
Manuscript revised August 9, 2004.
[†]The authors are with the Department of Electrical and Communication Engineering, Tohoku University, Sendai-shi, 980-8579 Japan.
a) E-mail: deep@mobile.ecei.tohoku.ac.jp

fixed as that attainable with an OFDM system. Data rate equivalent to the OFDM system can be realized with DS-CDMA by assigning all the available codes, equal to the spreading factor SF, to the same user, resulting in what is commonly referred to as multicode DS-CDMA [12]. In MC-CDMA with the same number of subcarriers as in OFDM, when the number of multiplexed codes is the same as SF, the transmission rate is the same as in OFDM. MC-CDMA with SF=1 is in fact the OFDM system. The comparison is first done for the uncoded system and the simulation results compared with the theoretical results. Then, the comparison is done with RCPT HARQ for various systems and propagation parameters. Higher level modulations like 16-quadrature amplitude modulation (QAM) and 64QAM are also considered.

The rest of the paper is organized as follows. Section 2 presents the transmission system model and also describes how the soft decision value necessary for turbo decoding is computed for DS-CDMA and MC-CDMA. The LLR computation and the MMSE weight for packet combining are introduced. The simulation results are presented and discussed in Section 3. Section 4 concludes the paper.

2. Transmission System Model

2.1 Overall System Model

The transmission system model is shown in Fig. 1. The transmitter consists of a CRC encoder, an RCPT encoder, a bit interleaver, and a data modulator followed by an OFDM, MC-CDMA or DS-CDMA transmitter. The CRC encoder adds the error detection parity check sequence to a binary data sequence to form a CRC encoded sequence $\{u_k\}$ of length K' which is input to the RCPT encoder. The rate 1/3 turbo encoder output sequences (the systematic bit sequence $\{u_k\}$ and the two parity bit sequences $\{p_k^{(1)}\}$ and $\{p_k^{(2)}\}$) are punctured according to the puncturing patterns of different RCPT HARQ schemes as described in Sect. 2.3 and the resulting sequences are buffered for possible retransmissions. The punctured sequence that is to be transmitted is bit interleaved and data-modulated. Let the data-modulated symbol sequence be $\{x(n)\}$ with $E[x(n)^2] = 1$, where $E[.]$ denotes the ensemble average operation. It is then transmitted as OFDM, MC-CDMA or DS-CDMA signal as described in the next sub-section.

The receiver consists of a data-demodulator, a bit deinterleaver, an RCPT decoder and a CRC decoder in addition to an OFDM, MC-CDMA or DS-CDMA specific receiver. The recovered symbol sequence $\{\hat{x}(n)\}$ is demodulated, deinterleaved and input to the RCPT decoder, where error correction is performed and the CRC coded sequence estimate $\{\hat{u}_k\}$ is obtained. If no error is detected, the CRC decoder outputs the received binary data sequence. In the case of errors being detected by the CRC decoder, a retransmission is requested.

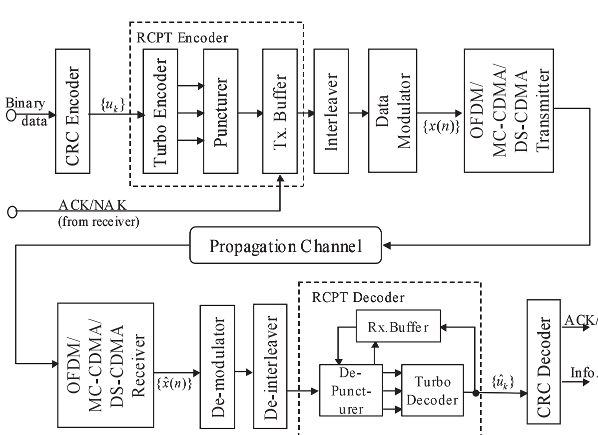

Fig. 1 Transmission system model.

2.2 Signaling Techniques

Three signaling techniques—multicode DS-CDMA, multicode MC-CDMA and OFDM—are considered. In an OFDM system, N_c symbols are transmitted using the N_c subcarriers over a duration of N_cT_s, T_s is the data modulated symbol length. In DS-CDMA and MC-CDMA, N_c symbols can be transmitted over a duration of N_cT_s when $C = SF$. However, time, frequency and code utilization differ among the schemes. Figure 2 shows how N_c data-modulated symbols are adjusted in each of the three signaling techniques.

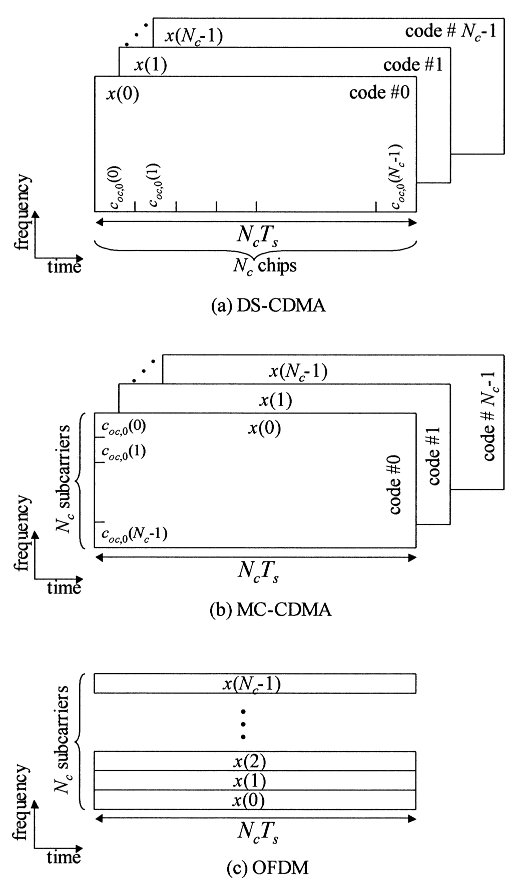

Fig. 2 Time, frequency and code utilization.

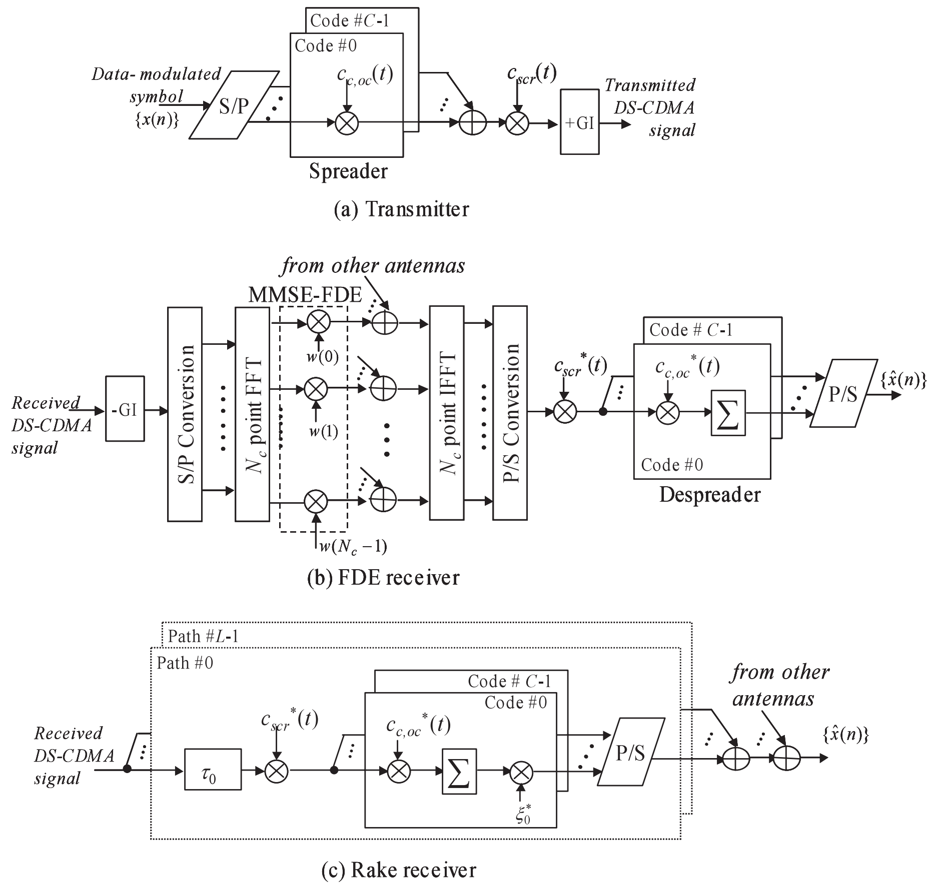

Fig. 3 Multicode DS-CDMA transmitter/receiver.

$SF = N_c$ for DS-CDMA and MC-CDMA. Guard interval (GI) is necessary for OFDM, MC-CDMA and also for DS-CDMA with FDE, but is omitted in Fig. 2 for simplicity.

2.2.1 DS-CDMA

The DS-CDMA transmitter/receiver structure is shown in Figs. 3(a)∼(c). The data-modulated symbol sequence $\{x(n)\}$ is serial-to-parallel (S/P) converted to C symbol streams $\{x_c(i),\ c = 0 \sim C-1,\ i = 0 \sim K-1\}$ and each symbol in the C streams is spread by an orthogonal code $\{c_{oc,c}(t),\ c = 0 \sim C-1,\ t = 0 \sim SF-1\}$, with spreading factor SF (C is called the code multiplex order and $C \leq SF$). The C chip sequences are then added and multiplied by a common scrambling code $\{c_{scr}(t)\}$. The resultant multicode chip sequence $s_{ds}(t)$ can be expressed in the equivalent low-pass representation as

$$s_{ds}(t) = \sqrt{\frac{2P}{SF}} \sum_{c=0}^{C-1} x_c(\lfloor t/SF \rfloor)\, c_{oc,c}(t \bmod SF) c_{scr}(t) \tag{1}$$

for $t = 0 \sim K\cdot SF-1$, where P represents the transmit power per code. In this paper, FDE is considered (see Fig. 3(b)). After insertion of the N_g-sample GI for every block of N_c chips [6], [7], where N_c is the number of fast Fourier transform (FFT) points and N_g is a fraction of N_c, the resultant GI-inserted signal $\{\tilde{s}(t); t = -N_g \sim N_c-1\}$ is transmitted over the propagation channel. Without loss of generality, we assume the transmission of the first block of $N_c + N_g$ chips for the explanation purpose of FFT and inverse FFT (IFFT) operations performed at the receiver.

The signal transmitted over a frequency selective fading channel is received by M antennas. The received multicode DS-CDMA signal on each antenna is sampled at the chip rate to obtain $\{\tilde{r}_m(t); t = -N_g \sim N_c-1 \text{ and } m = 0 \sim M-1\}$. The N_g-sample GI is removed and N_c-point FFT is applied to decompose the received DS-CDMA signal into the N_c frequency components. The kth frequency component for the received signal on the mth antenna is

$$\begin{aligned} R_m(k) &= \sum_{t=0}^{N_c-1} \tilde{r}_m(t) \exp\left(-j2\pi t \frac{k}{N_c}\right) \\ &= H_m(k)S(k) + \Pi_m(k) \end{aligned} \tag{2}$$

for $k = 0 \sim N_c-1$, where $H_m(k)$ and $\Pi_m(k)$ denote the channel gain and the noise component due to the additive white Gaussian noise (AWGN) at the kth frequency component for the mth receive antenna and $S(k)$ is the Fourier transform of the transmitted multicode DS-CDMA signal given by

$$S(k) = \sum_{t=0}^{N_c-1} s_{ds}(t) \exp\left(-j2\pi t \frac{k}{N_c}\right). \tag{3}$$

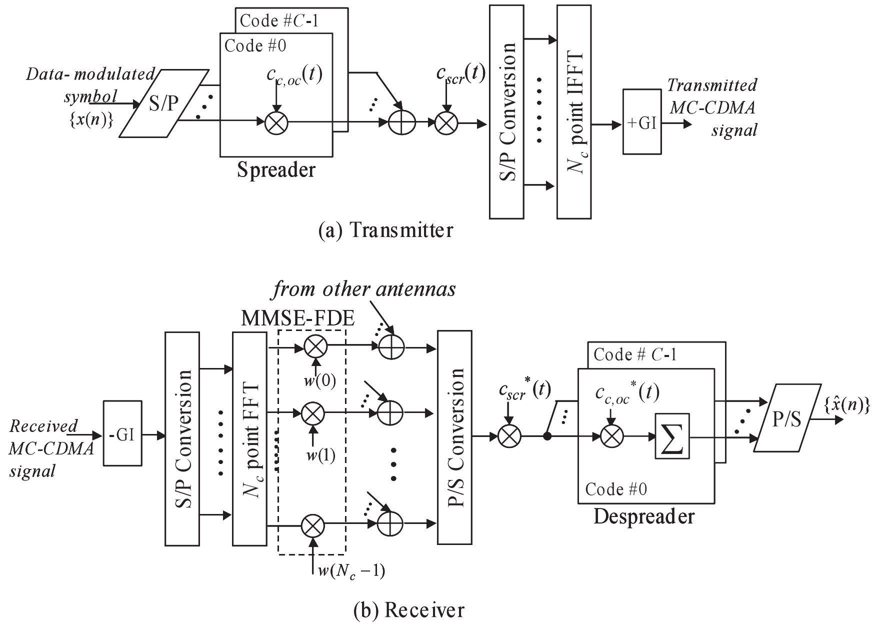

Fig. 4 Multicode MC-CDMA transmitter/receiver with FDE.

MMSE equalization based on minimizing the squared error for each frequency component is assumed. Joint antenna diversity and MMSE-FDE is carried out using the equalization weight $w_m(k)$ for $R_m(k)$ given by [7], [8]

$$w_m(k) = \frac{H_m^*(k)}{\sum_{m=0}^{M-1} |H_m(k)|^2 + \left[\frac{C}{SF}\frac{PT_s}{N_0}\right]^{-1}}, \tag{4}$$

where (.)* denotes the complex conjugate operation. After joint antenna diversity and MMSE-FDE, the signals from different antennas are added

$$R(k) = \sum_{m=0}^{M-1} w_m(k) R_m(k) \tag{5}$$

and IFFT is carried out to obtain the multicode DS-CDMA signal in the time-domain:

$$\hat{r}(t) = \frac{1}{N_c}\sum_{k=0}^{N_c-1} R(k)\exp\left(j2\pi k\frac{t}{N_c}\right) \tag{6}$$

for $t = 0 \sim N_c - 1$. IFFT is followed by despreading to obtain

$$\hat{x}_c(n) = \frac{1}{SF}\sum_{t=nSF}^{(n+1)SF-1} \hat{r}(t)\{c_{oc,c}(t \bmod SF)c_{scr}(t)\}^*, \tag{7}$$

for $n = 0 \sim N_c/SF - 1$ and $c = 0 \sim C-1$. $\{\hat{x}_c(n)\}$ is parallel-to-serial (P/S) converted to obtain $\{\hat{x}(n)\}$ for data demodulation. The soft decision values are generated using the LLR approximation (see Sect. 2.4). After all the data symbols are received, turbo decoding is performed with the LLR values.

Conventional DS-CDMA systems employ a rake combiner. The rake combiner consists of a correlator followed by a despreader and coherent detector for each path as shown in Fig. 3(c). The signals for all the paths are combined using the maximal ratio combining (MRC). It is shown in [13] that rake combining in the time-domain is equivalent to MRC equalization in the frequency-domain. For MRC, the equalization weight is

$$w_m(k) = H_m^*(k). \tag{8}$$

2.2.2 MC-CDMA and OFDM

In MC-CDMA, the spread signal is transmitted over a number of subcarriers. This is done by applying the IFFT. The MC-CDMA transmitter/receiver model is shown in Fig. 4. The code-multiplexing order for MC-CDMA is also taken to be C. The kth subcarrier component can be expressed using the equivalent low-pass representation as

$$s_{mc}(k) = \sqrt{\frac{2P}{SF}}\sum_{c=0}^{C-1} x_c(\lfloor k/SF \rfloor)\, c_{oc,c}(k \bmod SF)c_{scr}(k). \tag{9}$$

After IFFT, GI is inserted and the MC-CDMA signal is transmitted over a frequency selective fading channel. The received MC-CDMA signal is decomposed into the N_c orthogonal subcarrier components $\{R_m(k)\}$ by applying FFT after GI removal. The MMSE-FDE is carried out similar to Eq. (5) using the weight given by Eq. (4). After P/S conversion, frequency-domain despreading is applied to obtain

$$\hat{x}_c(n) = \frac{1}{SF}\sum_{k=nSF}^{(n+1)SF-1} R(k)\{c_{oc,c}(k \bmod SF)c_{scr}(k)\}^*, \tag{10}$$

for $n = 0 \sim N_c/SF - 1$ and $c = 0 \sim C - 1$. After P/S conversion, the sample sequence is demodulated using the LLR

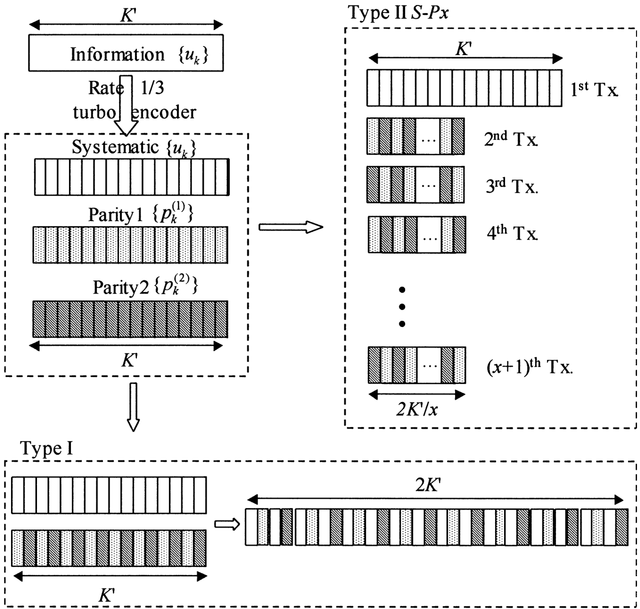

Fig. 5 Different RCPT HARQ schemes.

approximation as for DS-CDMA and then decoded after depuncturing.

OFDM system is equivalent to an MC-CDMA system with $SF = C = 1$. Since, SF=1, there is no frequency diversity and since C=1, no inter-code-interference (ICI) as well. Hence for OFDM, MRC weight, which maximizes the signal-to-noise ratio, given in Eq. (8) is the most suitable.

2.3 RCPT HARQ

Two types of HARQ schemes—type I and type II—are considered in this paper. The schematic diagrams are shown in Fig. 5. They are obtained by puncturing a rate 1/3 turbo code with different puncturing period P [9], [10].

(1) *Type I*: The two parity bit sequences $\{p_k^{(1)}\}$ and $\{p_k^{(2)}\}$, obtained after rate 1/3 turbo coding, are punctured with P=2 and transmitted along with the information sequence. In case a retransmission is requested, the same packet is transmitted and packet combining is employed using the updated MMSE-FDE weight as shown in Sect. 2.5.

(2) *Type II*: Three type II schemes are considered, represented by *S-Px* (systematic-puncture period $P = x$). $\{p_k^{(1)}\}$ and $\{p_k^{(2)}\}$ are punctured with $P = x$ and x different sequences of length $2K'/x$ are obtained, where K' is the CRC encoded sequence length. For the selection of the puncturing matrices, a heuristic approach is followed. For each puncturing period, the parity bit sequences are punctured such that the bits furthest apart in the two sequences are periodically selected. The puncturing matrices for the different schemes are as follows:

Puncturing matrices for S-$P2$ (binary notation):

$$\begin{bmatrix}1&1\\0&0\\0&0\end{bmatrix}\begin{bmatrix}0&0\\1&0\\0&1\end{bmatrix}\begin{bmatrix}0&0\\0&1\\1&0\end{bmatrix}$$

Puncturing matrices for S-$P4$ (binary notation):

$$\begin{bmatrix}1&1&1&1\\0&0&0&0\\0&0&0&0\end{bmatrix}\begin{bmatrix}0&0&0&0\\1&0&0&0\\0&0&1&0\end{bmatrix}\begin{bmatrix}0&0&0&0\\0&1&0&0\\0&0&0&1\end{bmatrix}\begin{bmatrix}0&0&0&0\\0&0&1&0\\1&0&0&0\end{bmatrix}\begin{bmatrix}0&0&0&0\\0&0&0&1\\0&1&0&0\end{bmatrix}$$

Puncturing matrices for S-$P8$ (octal notation):

$$\begin{bmatrix}3&7&7\\0&0&0\\0&0&0\end{bmatrix}\begin{bmatrix}0&0&0\\2&0&0\\0&1&0\end{bmatrix}\begin{bmatrix}0&0&0\\0&0&2\\0&4&0\end{bmatrix}\begin{bmatrix}0&0&0\\0&2&0\\0&0&1\end{bmatrix}\begin{bmatrix}0&0&0\\0&0&4\\1&0&0\end{bmatrix}\begin{bmatrix}0&0&0\\0&1&0\\2&0&0\end{bmatrix}$$
$$\begin{bmatrix}0&0&0\\1&0&0\\0&0&4\end{bmatrix}\begin{bmatrix}0&0&0\\0&0&1\\0&2&0\end{bmatrix}\begin{bmatrix}0&0&0\\0&4&0\\0&0&2\end{bmatrix}$$

In all the schemes, the first transmission consists of transmitting only the systematic bit sequence $\{u_k\}$ of length K'. The number of bits transmitted in the second transmission onwards differs depending on the puncturing period. After each retransmission, turbo decoding is performed. As the number of retransmissions increases, the resultant code rate decreases. For S-$P2$, the systematic bit sequence and the two parity bit sequences are received after 3 transmissions, whereas it takes 5 and 9 transmissions for S-$P4$ and S-$P8$, respectively. In all the schemes, incremental redundancy [14] and packet combing [15] (in case the same packet is retransmitted) with updated MMSE-FDE weight (see Sect. 2.5) are utilized.

2.4 LLR Computation for Turbo Decoding

The soft decision values for turbo decoding are obtained by computing the LLR for each bit. For computing the LLR from the received symbol $\hat{x}_c(n)$, we need to know the statistics of $\hat{x}_c(n)$. For DS-CDMA with MMSE-FDE, the multicode DS-CDMA signal in the time-domain after MMSE-FDE given by Eq. (6) can be expressed as

$$\begin{aligned}\hat{r}(t) &= \left(\frac{1}{N_c}\sum_{k=0}^{N_c-1}\tilde{H}(k)\right)s_{ds}(t)\\ &\quad + \frac{1}{N_c}\sum_{k=0}^{N_c-1}\tilde{H}(k)\sum_{\substack{\tau=0\\ \neq t}}^{N_c-1}s_{ds}(\tau)\exp\left(j2\pi k\frac{t-\tau}{N_c}\right)\\ &\quad + \tilde{\eta}_{ds}(t) \end{aligned}\tag{11}$$

where

$$\begin{cases}\tilde{H}(k) = \displaystyle\sum_{m=0}^{M-1}H(k)w(k)\\ \tilde{\eta}_{ds}(t) = \displaystyle\frac{1}{N_c}\sum_{k=0}^{N_c-1}\tilde{\Pi}(k)\exp\left(j2\pi k\frac{t}{N_c}\right)\end{cases}. \tag{12}$$

In Eq. (11), the first term is the desired chip sequence, the second the ICI and the third the noise due to AWGN. It is seen that the equivalent channel gain for each chip is $\frac{1}{N_c}\sum_{k=0}^{N_c-1}\tilde{H}(k)$ and benefits from full frequency diversity gain. Hence $\hat{x}_c(n)$ of Eq. (7) can be expressed as

$$\hat{x}_c(n) = \sqrt{\frac{2P}{SF}}\left(\frac{1}{N_c}\sum_{k=0}^{N_c-1}\tilde{H}(k)\right)x_c(n) + \mu^{ds}_{ICI}(n) + \mu^{ds}_{noise}(n). \tag{13}$$

The first term represents the desired data symbol component and the second and third terms, $\mu^{ds}_{ICI}(n)$ and $\mu^{ds}_{noise}(n)$, are ICI and the noise due to AWGN, respectively, given by

$$\begin{aligned}\mu^{ds}_{ICI}(n) &= \frac{1}{SF}\sum_{t=nSF}^{(n+1)SF-1}\{c_{oc,c}(t \bmod SF)c_{scr}(t)\}^* \\ &\quad\times\frac{1}{N_c}\sum_{k=0}^{N_c-1}\tilde{H}(k)\left[\sum_{\substack{\tau=0\\ \neq t}}^{N_c-1}s(\tau)\exp\left(j2\pi k\frac{t-\tau}{N_c}\right)\right] \\ \mu^{ds}_{noise}(n) &= \frac{1}{SF}\sum_{t=nSF}^{(n+1)SF-1}\{c_{oc,c}(t \bmod SF)c_{scr}(t)\}^*\tilde{\eta}_{ds}(t).\end{aligned} \tag{14}$$

In the case of MC-CDMA, the kth subcarrier component obtained after joint antenna diversity and MMSE-FDE is

$$R(k) = \tilde{H}(k)s_{mc}(k) + \tilde{\Pi}(k) \tag{15}$$

for $k = 0 \sim N_c - 1$. $\hat{x}_c(n)$ of Eq. (10) can be expressed as

$$\hat{x}_c(n) = \sqrt{\frac{2P}{SF}}\left(\frac{1}{SF}\sum_{k=nSF}^{(n+1)SF-1}\tilde{H}(k)\right)x_c(n) + \mu^{mc}_{ICI}(n) + \mu^{mc}_{noise}(n). \tag{16}$$

As for the DS-CDMA, the first term represents the desired signal component and the second and third terms are the ICI and the noise due to AWGN respectively. $\mu^{mc}_{ICI}(n)$ and $\mu^{mc}_{noise}(n)$ are given by

$$\begin{aligned}\mu^{mc}_{ICI}(n) &= \frac{1}{SF}\sqrt{\frac{2P}{SF}}\sum_{k=nSF}^{(n+1)SF-1}\{c_{oc,c}(k \bmod SF)c_{scr}(k)\}^* \\ &\quad\times\tilde{H}(k)\sum_{\substack{c'=0\\ \neq c}}^{C-1}x'_c(k)\{c_{oc,c'}(k \bmod SF)c_{scr}(k)\} \\ \mu^{mc}_{noise}(n) &= \frac{1}{SF}\sum_{k=nSF}^{(n+1)SF-1}\{c_{oc,c}(k \bmod SF)c_{scr}(k)\}^*\tilde{\Pi}(k).\end{aligned} \tag{17}$$

The equivalent channel gain for each symbol is $\frac{1}{SF}\sum_{k=nSF}^{(n+1)SF-1}\tilde{H}(k)$ and, unlike DS-CDMA, the frequency diversity gain is a function of SF.

In summary, the received symbol for code c is given by

$$\hat{x}_c(n) = \hat{H}(n)x_c(n) + \mu(n)$$

$$= \begin{cases}\sqrt{\frac{2P}{SF}}\left(\frac{1}{N_c}\sum_{k=0}^{N_c-1}\tilde{H}(k)\right)x_c(n) + \mu^{ds}_{ICI}(n) + \mu^{ds}_{noise}(n) & \text{for DS-CDMA} \\ \sqrt{\frac{2P}{SF}}\left(\frac{1}{SF}\sum_{k=nSF}^{(n+1)SF-1}\tilde{H}(k)\right)x_c(n) + \mu^{mc}_{ICI}(n) + \mu^{mc}_{noise}(n) & \text{for MC-CDMA}\end{cases}, \tag{18}$$

where $\hat{H}(n)$ is the equivalent channel gain for the symbol $x_c(n)$. The noise plus ICI is approximated as a zero-mean complex Gaussian noise variable $\mu(n)$ with variance $2\sigma^2$. Hence, the LLR for the bth bit in $\hat{x}_c(n)$ is given by

$$L(b) = \ln\frac{\sum_{\{\hat{s}:b=1\}}\frac{1}{\sqrt{2\pi\sigma^2}}\exp\left(-\frac{1}{2\sigma^2}\left|\hat{x}_c(n) - \sqrt{\frac{2P}{SF}}\hat{H}(n)\hat{s}\right|^2\right)}{\sum_{\{\hat{s}:b=0\}}\frac{1}{\sqrt{2\pi\sigma^2}}\exp\left(-\frac{1}{2\sigma^2}\left|\hat{x}_c(n) - \sqrt{\frac{2P}{SF}}\hat{H}(n)\hat{s}\right|^2\right)}, \tag{19}$$

where $\{\hat{s}\}$ are the candidate symbols with the bth bit as 0 or 1. From [11], we approximate the denominator and numerator within the bracket of Eq. (19) as

$$\begin{aligned}&\sum_{\{\hat{s}:b=1\text{ or }0\}}\frac{1}{\sqrt{2\pi\sigma^2}}\exp\left(-\frac{1}{2\sigma^2}\left|\hat{x}_c(n) - \sqrt{\frac{2P}{SF}}\hat{H}(n)\hat{s}\right|^2\right) \\ &\approx \max_{\{\hat{s}:b=1\text{ or }0\}}\frac{1}{\sqrt{2\pi\sigma^2}}\exp\left(-\frac{1}{2\sigma^2}\left|\hat{x}_c(n) - \sqrt{\frac{2P}{SF}}\hat{H}(n)\hat{s}\right|^2\right).\end{aligned} \tag{20}$$

Representing

$$\begin{aligned}&\max_{\{\hat{s}:b=1\text{ or }0\}}\frac{1}{\sqrt{2\pi\sigma^2}}\exp\left(-\frac{1}{2\sigma^2}\left|\hat{x}_c(n) - \sqrt{\frac{2P}{SF}}\hat{H}(n)\hat{s}\right|^2\right) \\ &= \frac{1}{\sqrt{2\pi\sigma^2}}\exp\left(-\frac{1}{2\sigma^2}\left|\hat{x}_c(n) - \sqrt{\frac{2P}{SF}}\hat{H}(n)\hat{s}_{1\text{ or }0,\max}\right|^2\right)\end{aligned} \tag{21}$$

we can write the LLR as

$$L(b) = \frac{1}{2\sigma^2}\left(\left|\hat{x}_c(n) - \sqrt{\frac{2P}{SF}}\hat{H}(n)\hat{s}_{0,\max}\right|^2 - \left|\hat{x}_c(n) - \sqrt{\frac{2P}{SF}}\hat{H}(n)\hat{s}_{1,\max}\right|^2\right). \tag{22}$$

Therefore, the LLR for DS-CDMA and MC-CDMA can be computed using $\hat{H}(n)$ and σ^2 given by [8]

$$\hat{H}(n) = \begin{cases}\frac{1}{N_c}\sum_{k=0}^{N_c-1}\tilde{H}(k) & \text{for DS-CDMA} \\ \frac{1}{SF}\sum_{k=nSF}^{(n+1)SF-1}\tilde{H}(k) & \text{for MC-CDMA}\end{cases} \tag{23}$$

and

$$\sigma^2 = \begin{cases} \dfrac{1}{SF}\dfrac{N_0}{T_s}\left[\begin{array}{l} \dfrac{1}{N_c}\displaystyle\sum_{k=0}^{N_c-1}\sum_{m=0}^{M-1}|w_m(k)|^2 + \left(\dfrac{C}{SF}\dfrac{PT_s}{N_0}\right) \\ \cdot\left\{\dfrac{1}{N_c}\displaystyle\sum_{k=0}^{N_c-1}\left|\tilde{H}(k)\right|^2 - \left|\dfrac{1}{N_c}\displaystyle\sum_{k=0}^{N_c-1}\tilde{H}(k)\right|^2\right\} \end{array}\right] \\ \quad \text{for DS-CDMA} \\ \dfrac{1}{SF}\dfrac{N_0}{T_s}\left[\begin{array}{l} \dfrac{1}{SF}\displaystyle\sum_{k=nSF}^{(n+1)SF-1}\sum_{m=0}^{M-1}|w_m(k)|^2 \\ +\left(\dfrac{C-1}{SF}\dfrac{PT_s}{N_0}\right)\left\{\dfrac{1}{SF}\displaystyle\sum_{k=nSF}^{(n+1)SF-1}\left|\tilde{H}(k)\right|^2 \right. \\ \left. -\left|\dfrac{1}{SF}\displaystyle\sum_{k=nSF}^{(n+1)SF-1}\tilde{H}(k)\right|^2\right\} \end{array}\right] \\ \quad \text{for MC-CDMA.} \end{cases} \tag{24}$$

These LLR values are computed for $c = 0 \sim C-1$ and for all the bits in the symbol (2, 4 and 6 for QPSK, 16QAM and 64QAM, respectively).

2.5 Packet Combining for MMSE-FDE

For all the HARQ schemes used in this paper, packet combining is employed if the same packet is transmitted more than once. For type I HARQ, packet combining is carried out with each retransmission. For type II HARQ, incremental redundancy [14] is employed until rate 1/3 code is received. If further transmissions are needed, packet combining is utilized. For example, with type II HARQ S-$P2$, the code rate is reduced for the second and third transmissions. However if a fourth transmission is requested, the first and the fourth packets contain the same symbols and packet combining is utilized. When the same packet is retransmitted, time diversity gain is obtained, similar to antenna diversity [16], so the weight for MMSE-FDE needs to be modified to take advantage of the time diversity. Therefore, we propose to use the MMSE weights for packet combining as

$$w_{m,tr}(k) = \frac{H^*_{m,tr}(k)}{\displaystyle\sum_{tr=0}^{Tr-1}\sum_{m=0}^{M-1}\left|H_{m,tr}(k)\right|^2 + \left[\frac{C}{SF}\frac{PT_s}{N_0}\right]^{-1}}, \tag{25}$$

where Tr is the number of times the same packet is received and $H_{m,tr}(k)$ is the channel gain at the kth frequency component for the tr-th transmission. In the results presented later, the modified MMSE weight for packet combining is used when the same packet is retransmitted.

3. Simulation Results and Discussions

3.1 Simulation Conditions

The simulation conditions are summarized in Table 1. The turbo encoder/decoder parameters [17] are as shown in Table 2. The information sequence length K'=1024 bits (CRC encoded sequence length is treated as the information sequence length). The channel interleaver used in the simulation is a size $2^a \times 2^b$ block interleaver, where a and b are the maximum allowable integers for a given sequence size and are determined so that an interleaver as close as possible to a square interleaver can be obtained. Ideal coherent QPSK data modulation/demodulation is assumed, unless otherwise stated. Walsh-Hadamard (WH) codes are used as orthogonal codes and a long pseudo noise (PN) code is used as the scramble sequence. The number N_c of subcarriers (the number of FFT points) for MC-CDMA (DS-CDMA) is taken to be N_c=256 with a GI of N_g=32. Unless otherwise stated, SF=256 for both DS-CDMA and MC-CDMA.

It is assumed that the propagation channel has L discrete paths having chip-spaced (or FFT sample spaced) different time delays and experiencing independent Rayleigh fading. The channel impulse response $\xi(t,\tau)$ at time t can be expressed as [18], [19]

$$\xi(t,\tau) = \sum_{l=0}^{L-1}\xi_l(t)\delta(\tau-\tau_l), \tag{26}$$

where $\xi_l(t)$ and τ_l denote the complex path gain at time t and the time delay of the lth path, respectively, with

Table 1 Simulation conditions.

Information sequence length	K'=1024 bits	
Channel code	Rate 1/3 turbo code	
Channel interleaver	Block interleaver	
Data modulation	Coherent QPSK,16QAM, 64QAM	
Signaling technique	Spreading code	WH codes and a long PN code
	Multicode DS-CDMA/ OFDM/ Multicode MC-CDMA	No. of subcarriers/ FFT points N_c=256
		GI : N_g=32
		Spreading factor SF=1~256
Channel model	Data channel	Rayleigh fading $\tau_l = l$ (l=0~15) f_DT_{blk} = 0.001
	ARQ channel	Ideal
ARQ	Number of retransmissions	∞
	Type	Basic, type I, type II

Table 2 Turbo encoder/decoder parameters.

Encoder	Rate	1/3
	Component encoder	(13, 15) RSC
	Interleaver	S-random (S=$K^{1/2}$)
Decoder	Component decoder	Log-MAP
	Number of iterations	8

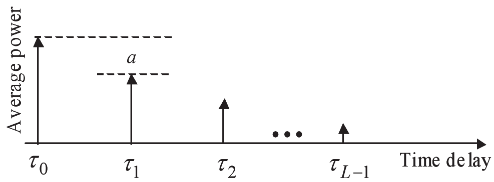

Fig. 6 Power delay profile.

$E\left[\sum_{l=0}^{L-1}|\xi_l(t)|^2\right] = 1$, here $E[.]$ denotes the ensemble average operation and $\delta(.)$ denotes the delta function. $\{\xi_l(t); l = 0 \sim L-1\}$ are independent zero-mean complex Gaussian processes. The power delay profile is shown in Fig. 6. $E[|\xi_l(t)|^2]$, $l = 0 \sim L-1$, are assumed to be exponentially decreasing with decay factor α. When α=0 dB, we get a uniform power delay profile with the average power per path equal to $1/L$. In the following simulations, L=16 is assumed. Uncorrelated, slow L=16-path Rayleigh faded paths are generated using Dent's model [20]. The time delay $\tau_l = l$, $l = 0 \sim 15$, is assumed. We have assumed block fading, where the path gains stay constant over one data block (the block length in time equals $T_{blk}=(N_c + N_g)T_c$), with T_c denoting the chip or sample duration. The normalized maximum Doppler frequency f_DT_{blk}=0.001 and the decay factor of the power delay profile α=0 dB (uniform power delay profile) are assumed unless otherwise stated. f_DT_{blk}=0.001 corresponds to a mobile velocity of about 100 km/hr when the carrier frequency is 5 GHz and the transmission rate is 100M symbols/sec. For DS-CDMA with rake combining, ideal 16-finger rake combiner is assumed. For all the signaling techniques, channel estimation is assumed to be ideal. An error-free feedback channel and ideal error detection for ARQ control are assumed. The number of retransmissions is taken to be infinite.

In the paper, for type II HARQ, the parity check packet is shorter than the systematic (information) bit packet. We assume dynamic frame structure, i.e., the frame length is varied depending on the number of bits transmitted. The data to be transmitted is divided into several packets, and they are transmitted using parallel independent stop-and-wait (SW) ARQ processes [21] so that the transmission channel can be kept occupied all the time. Analysis of the throughput can be dealt with as a single ARQ process.

The throughput in bits per sec per Hertz (bps/Hz) is defined here as the ratio of the number of information bits transmitted successfully to the total number of bits transmitted times the transmission rate normalized by the 3 dB bandwidth. In MC-CDMA, OFDM and DS-CDMA with MMSE-FDE, the insertion of GI is necessary. For the same transmission rate, the bandwidth is increased by a factor of $(1+N_g/N_c)$. On the other hand, if the bandwidth expansion is not allowed the transmission rate should be lowered by a factor of $(1+N_g/N_c)$. For both the cases, therefore, the maximum throughput attainable is the same and is 1.8 bps/Hz, 3.6 bps/Hz and 5.3 bps/Hz for QPSK, 16QAM and 64QAM, respectively. For DS-CDMA with rake combining, GI is not needed and the maximum attainable throughput is 2 bps/Hz, 4 bps/Hz and 6 bps/Hz for QPSK, 16QAM and 64QAM, respectively.

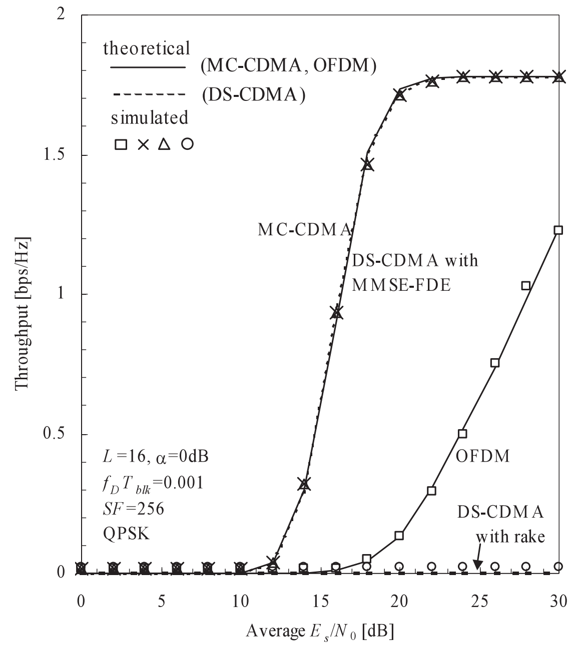

Fig. 7 Unocded ARQ throughput (theoretical vs. simulation result).

In this paper, we have not considered the transmit filter for DS-CDMA. The well-known square-root Nyquist filter with roll-off factor ρ can be used at both the transmitter and receiver for bandwidth restriction. The ideal brick-wall filter is when ρ=0 to achieve the bandwidth of $1/T_c$. In this paper, we assume ρ=0 in the simulation and all the throughput performances are plotted for ρ=0. However, in practical cases, $\rho = 0.2 \sim 0.5$ is used; the bandwidth is larger than MC-CDMA and OFDM by a factor of 1+ρ and therefore, the throughput in bps/Hz reduces by a factor of 1+ρ. However, the 3 dB bandwidth is the same for all the systems and if the throughput is defined, as in the paper, using the 3 dB bandwidth, it is the same for all ρ.

3.2 Uncoded ARQ

In Fig. 7, the throughput of uncoded ARQ is plotted as a function of the average received signal energy per symbol-to-noise power spectrum density ratio, $E_s/N_0 = PT_s(1+N_g/N_c)$, for DS-CDMA, MC-CDMA and OFDM. $SF=C$=256 is assumed for DS- and MC-CDMA. For the uncoded case, the throughput is theoretically evaluated in Appendix. The theoretical results obtained from Eqs. (A· 1)–(A· 5) by Monte-Carlo numerical computation method are plotted as solid and dotted curves. The results obtained from computer simulations are plotted by various marks. It is seen that the simulation results coincide with the theoretical results. This confirms the validity of the simulation results. It is seen that the throughput of DS-CDMA with MMSE-FDE is the same as that for MC-CDMA and is better than that of OFDM. In OFDM, there is no frequency diversity gain and hence the first transmission is not sufficient for error free transmission for most cases. The throughput for DS-CDMA with rake combining is almost zero since, in a frequency selective channel, the code orthogonality is severely destroyed.

3.3 Performance Comparison of Different HARQ Schemes

The throughput of the different HARQ schemes described in Sect. 2.3 is plotted as a function of the average received E_s/N_0 in Figs. 8(a) and (b) when L=16 and α=0 dB. SF=C=256 is assumed. The throughput of DS-CDMA with rake combining and MMSE-FDE are plotted in Fig. 8(a) and that of MC-CDMA and OFDM are plotted in Fig. 8(b). Type I HARQ scheme has better throughput than when no coding is applied, however as the redundancy bits equal to the number of information bits are always transmitted, the throughput is always less than 1 bps/Hz. Among the type II HARQ schemes, the highest throughput is attained with the type II HARQ S-P8 scheme for all the signaling techniques. The number of bits transmitted in the second transmission onwards is less for the S-P8 scheme; the transmission of unnecessary redundant bits is avoided and the throughput is seen to be better than either the type II HARQ S-P2 or S-P4 scheme. From Fig. 8(a), it can be observed that for all types of HARQ, MMSE-FDE provides a higher throughput than rake combining. When multiple codes are multiplexed, the code orthogonality is destroyed in a frequency selective channel. For a coded system, there is a tradeoff between frequency diversity gain due to the spreading of symbols, coding gain due to a better frequency interleaving effect and orthogonality destruction among the codes in a frequency selective channel. MMSE-FDE can restore the code orthogonality to a certain extent. We see from Fig. 8(b) that the type I HARQ throughput is same for MC-CDMA and OFDM. OFDM also benefits from a coding gain as redundancy bits are transmitted together with the information bits resulting in an improved throughput. For type II HARQ, using MC-CDMA is better than using OFDM. In OFDM, SF=C=1 so there is no orthogonality destruction but also no frequency diversity gain. However, with channel coding, coding gain due to better frequency interleaving can be obtained. It should be noted that there is no parity bit in the first transmission and no coding gain for OFDM; hence the throughput for type II HARQ using OFDM is inferior to that using MC-CDMA. If we compare the throughput in Figs. 8(a) and (b), we see that using DS-CDMA with MMSE-FDE is the same as that using MC-CDMA and is better than using either OFDM or DS-CDMA with rake combining.

3.4 Effect of Spreading Factor

The throughput of DS-CDMA and MC-CDMA when $SF \leq N_c$ is plotted in Fig. 9 for C=SF. For reference, the throughput of DS-CDMA with rake combining is also plotted. The

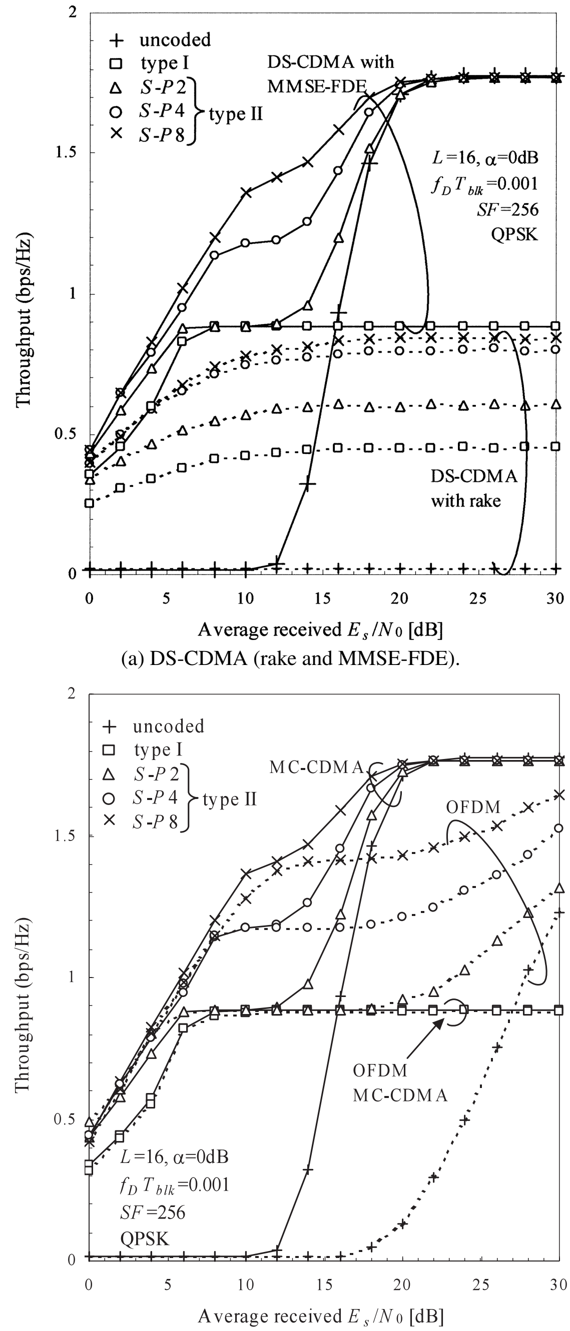

(a) DS-CDMA (rake and MMSE-FDE).

(b) OFDM and MC-CDMA.

Fig. 8 Throughput for different HARQ schemes.

throughput of uncoded DS-CDMA with rake combing is almost zero for all SF. For uncoded MC-CDMA, it is seen that the throughput increases with the increase in SF due to the increase in the frequency diversity effect and the highest throughput is obtained when SF=N_c=256. SF=1 corresponds to OFDM, and the throughput is almost zero due to no frequency diversity effect. For DS-CDMA with MMSE-FDE, the frequency diversity effect is not a function of SF but the frequency selectivity of the channel; full diversity gain is obtained for all SF. However it is seen that the

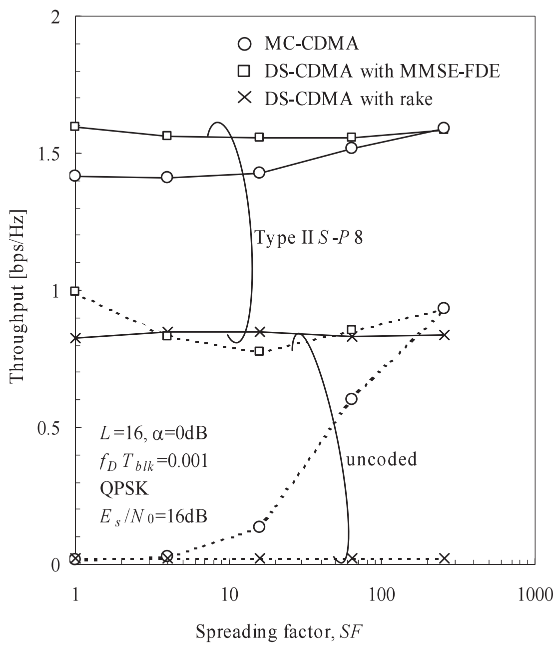

Fig. 9 Throughput for different spreading factor.

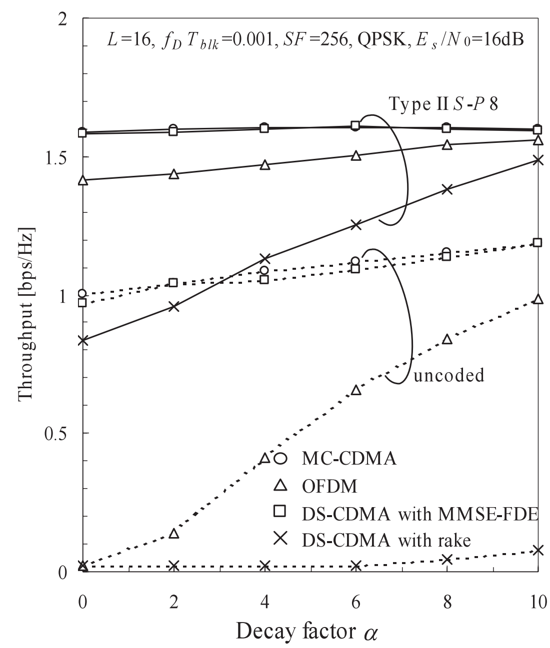

Fig. 10 Throughput as a function of α for type II HARQ S-P8.

throughput is a little lower for SF=16. Possible reason for this is given below. Since WH code has a periodic correlation property, a large ICI occurs after despreading as SF increases when C=SF. However, when PN code is used as the scramble sequence, contribution of the periodic correlation property of WH codes can be better suppressed as the ICI approaches the Gaussian process. This means that a large ICI rarely occurs after despreading as SF increases. Because of these two trade-off relations, the performance is seen to be worst for SF=16. With coding, the throughput is higher but almost independent of SF. For type II HARQ S-P8 using MC-CDMA, coding gain owing to better interleaving is obtained even for SF=1 (OFDM), but the throughput when SF=N_c is still the highest since, as said earlier, only frequency diversity gain is expected (no coding gain is present) at the first transmission. On the other hand, in DS-CDMA, full diversity gain is obtained for all SF. With type II HARQ S-P8, throughput is the same irrespective of SF for DS-CDMA due to the strong error correction capability of turbo code. The throughput using DS-CDMA with MMSE-FDE is the same as that using MC-CDMA for SF=N_c and is the highest for all $SF < N_c$.

3.5 Effect of Channel Selectivity

The frequency selectivity of the channel is a function of the decay factor α and the time delay separation $\Delta\tau$ between adjacent paths. The throughput is plotted as a function of the decay factor α in Fig. 10. As α decreases, the uncoded ARQ throughput decreases for all the signaling techniques due to the increased frequency selectivity. For multicode DS-CDMA and MC-CDMA, the orthogonality destruction is severer with higher selectivity, resulting in the reduction of throughput. Throughput using OFDM decreases due to increased packet errors owing to random errors. Throughput using DS-CDMA with rake combining is very low even for a channel with low frequency selectivity. For type II HARQ S-P8, the throughput using DS-CDMA with rake combining is seen to improve for high α due to coding gain in addition to less orthogonality destruction. As said earlier, there are more random errors in a channel with lower α, and random errors are desirable for turbo coding. Hence, for OFDM, MC-CDMA and DS-CDMA with MMSE-FDE, the dependence of the type II HARQ S-P8 throughput on the frequency selectivity of the channel is less.

The throughput is plotted as a function of the time delay separation $\Delta\tau$ between adjacent paths in Fig. 11. Since, N_g=32 is used, the maximum time delay exceeds the GI length when $\Delta\tau > 2$ and hence, the performance degrades for all the systems. For rake combining there is no GI, and the performance is independent of $\Delta\tau$. For an uncoded ARQ system, the throughput decreases drastically for $\Delta\tau > 2$. However, for type II HARQ S-P8, the throughput decreases gradually due to the powerful turbo coding.

The normalized maximum Doppler frequency $f_D T_{blk}$ is the measure of the channel's time selectivity. $f_D T_{blk}$ increases with the increase in the moving speed of the mobile terminal. The effect of $f_D T_{blk}$ on the throughput of type II HARQ S-P8 is plotted in Fig. 12. The maximum value is taken to be $f_D T_{blk}$=0.01, which corresponds to a vehicular speed as high as 200 km/hr when the carrier frequency is 5 GHz and the data rate is about 20 Mbps. For higher data rate and lower mobile velocity, $f_D T_{blk}$ is lower. Hence, $f_D T_{blk}$=0.01 is a realistic assumption even for high mobility users. For this value, the block fading assumption is valid [22]. For reference, the throughput for uncoded ARQ is also plotted. For the uncoded case, the throughput de-

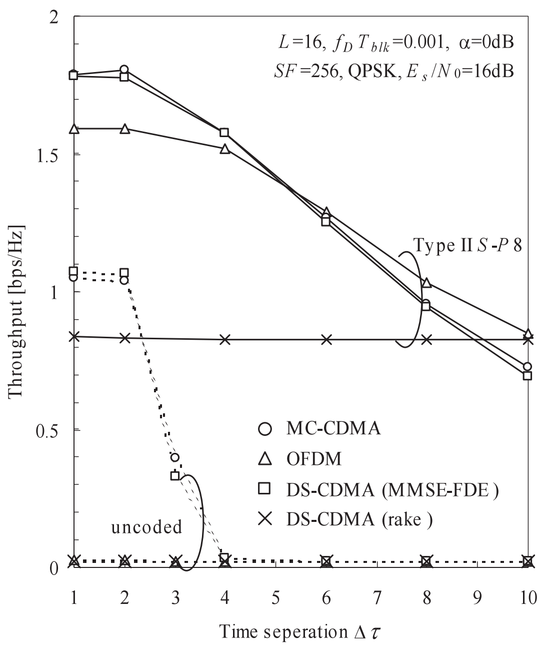

Fig. 11 Throughput as a function of the time separation $\Delta\tau$ between adjacent path type II HARQ S-P8.

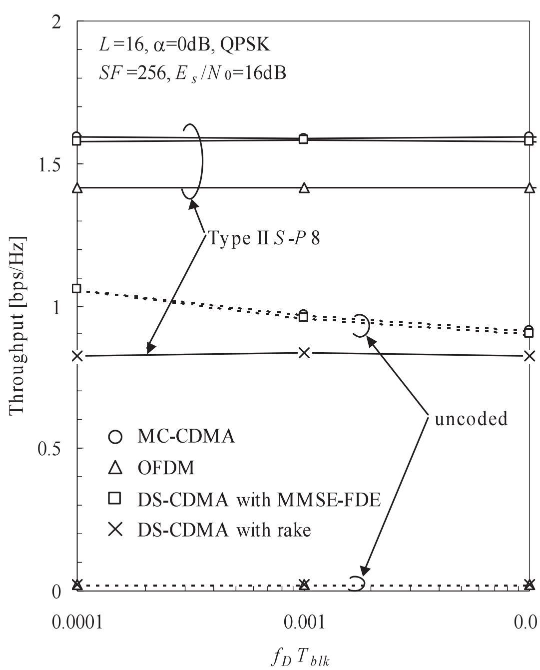

Fig. 12 Throughput as a function of $f_D T_{blk}$.

creases with the increase in the time selectivity. However for the type II HARQ S-P8, the throughput is seen to be almost independent of the time selectivity of the channel. This is because the packet errors increase with the increase in the time selectivity of the channel, but at the same time, the coding gain also increases due to better interleaving. Hence the throughput is almost independent of the time selectivity of the channel.

3.6 Effect of Higher Level Modulation

The number of bits that can be transmitted with each transmission can be increased with the modulation level. With 16QAM and 64QAM, 4 and 6 bits can be transmitted over each symbol. However, the BER worsens as the Euclidean distance between the symbols in the signal-space diagram reduces with the increase in the modulation level. It is shown in [23] that for higher level modulation, OFDM has a better BER performance than MC-CDMA and DS-CDMA with MMSE-FDE. The effect of modulation level on the throughput is plotted in Figs. 13(a) and (b) for type I HARQ and Type II HARQ S-P8, respectively. It is interesting to note two things: first the comparison among the modulation schemes and second the comparison among the signaling techniques for each modulation level. In Fig. 13(a), it is seen that for lower E_s/N_0 region, where noise is the predominant cause of packet errors, the throughput of type I HARQ is the highest when QPSK modulation is used. As E_s/N_0 increases, the 16QAM gives a better throughput and for $E_s/N_0 > 15$ dB, 64QAM gives the highest throughput. This is true for OFDM, MC-CDMA and also DS-CDMA with MMSE-FDE. However, if we compare the three signaling techniques, it is seen that for the region where QPSK modulation gives the highest throughput, all the schemes have the same throughput. But for 16QAM and 64QAM, OFDM provides a higher throughput. This is because for higher level modulation, the orthogonality destruction among the codes is severer, which results in the performance degradation of MC-CDMA and DS-CDMA. In OFDM, there is no code multiplexing and a large frequency diversity gain can be attained for a coded system owing to better interleaving, resulting in better throughput performance than either MC- or DS-CDMA.

Similar result is seen in Fig. 13(b), which plots the throughput of type II HARQ S-P8. However for high E_s/N_0, the throughput performance is seen to be better using MC-CDMA and DS-CDMA than OFDM. This can be explained as follows. For OFDM, there is no frequency diversity gain. Since no parity bit is transmitted in the first transmission, there is no coding gain for OFDM and a retransmission is requested. However for MC- and DS-CDMA, there is a large frequency diversity gain due to spreading and hence for very high E_s/N_0 values, retransmission may not be necessary. Thus for all the modulation schemes, the throughput is higher when MC- and DS-CDMA is used than OFDM for high E_s/N_0 value.

For OFDM, there is no frequency diversity gain, so the type II HARQ without redundancy in the first transmission is not desirable. Selecting the HARQ scheme suitable for OFDM is left as an interesting future study.

3.7 Antenna Diversity Reception

So far, we have considered a single antenna at the receiver. Recently using multiple antennas has been looked upon as

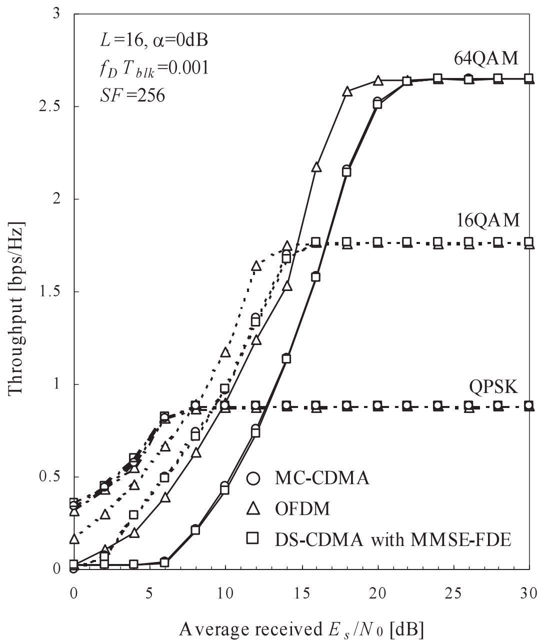

(a) Type I HARQ.

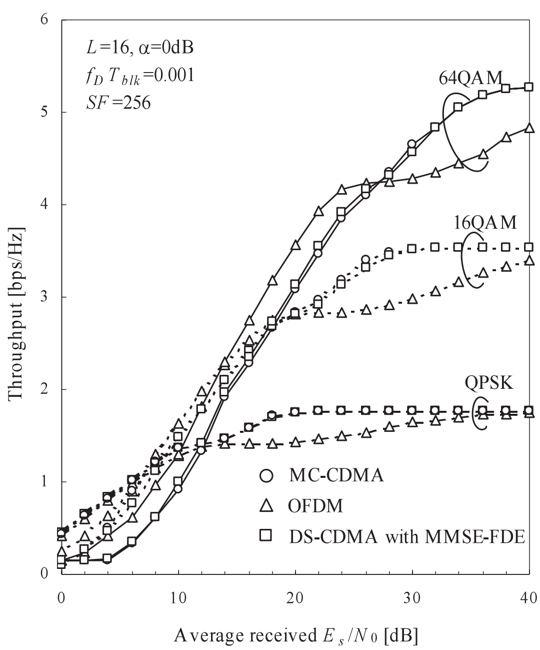

(b) Type II HARQ S-$P8$.

Fig. 13 Throughput with higher level modulation.

a desirable technique to improve throughput. When M antennas are used at the receiver, the signals received by M antennas are coherently combined using MRC scheme for OFDM. In DS-CDMA and MC-CDMA, both with FDE, joint antenna diversity and MMSE-FDE is performed [7], [16].

Figure 14 plots the effect of using two antennas at the receiver for type II HARQ S-$P8$ with QPSK and 16QAM. It is seen that the throughput can be significantly improved with antenna diversity reception. For QPSK, MC-CDMA

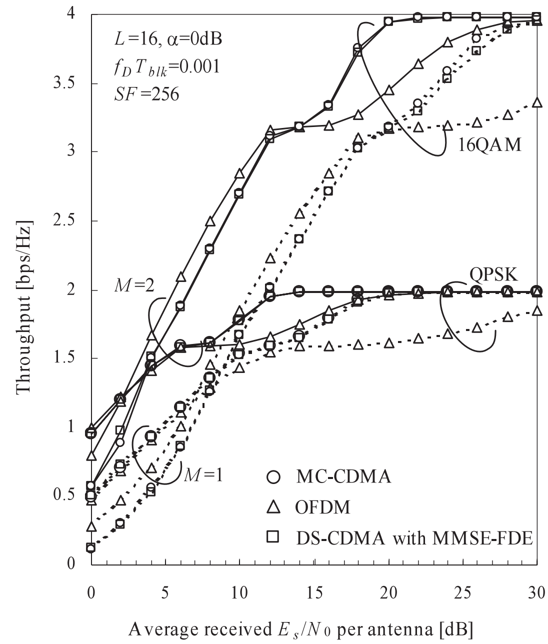

Fig. 14 Throughput with receive antenna diversity for type II HARQ S-$P8$.

and DS-CDMA provide a higher throughput than OFDM even in the presence of two antenna diversity reception. For 16QAM also, the presence of antenna diversity improves the throughput compared to a single receive antenna, but similar to the case of M=1, OFDM provides higher throughput in low E_s/N_0 region and MC- and DS-CDMA provide higher throughput in high E_s/N_0 region.

4. Conclusion

Throughput comparison of RCPT HARQ schemes in OFDM, multicode MC-CDMA and multicode DS-CDMA with MMSE-FDE and rake combining was performed. The LLR computation for turbo decoding was presented for MC-CDMA and DS-CDMA with MMSE-FDE. In addition, the MMSE weight for packet combining was introduced.

It was found that in a frequency selective fading channel, the throughput of HARQ using DS-CDMA with MMSE-FDE is much higher than that with rake combining due to partial orthogonality restoration by MMSE-FDE. The DS-CDMA throughput with MMSE-FDE is same as that using MC-CDMA when SF=N_c, but higher than MC-CDMA for $SF < N_c$, including OFDM (SF=1). However with higher level modulation, the type I HARQ throughput using OFDM is the highest due to large coding gain in OFDM and severe orthogonality destruction in DS-CDMA and MC-CDMA. For the type II HARQ, however, with no redundancy in the first transmission, DS-CDMA and MC-CDMA (SF=N_c) give higher throughput. It was also found that the use of antenna diversity reception improves the throughput for all the signaling techniques.

Orthogonal multicode approach has been considered for MC- and DS-CDMA in order to achieve the same data rate as in OFDM. In a frequency selective channel, the transmission performance of multicode DS-CDMA with rake combining significantly degrades due to severe ICI resulting from orthogonality destruction. Therefore, in this paper, MMSE-FDE was applied instead of rake combining to improve the performance. Another approach is to use interference cancellation. Interference cancellation can be applied to improve the performance for MC- and DS-CDMA systems. However, in this paper, interference cancellation has not been considered and left as an interesting future study. In this paper, symbol timing, channel estimation and feedback channel and error detection for ARQ have been assumed to be ideal. It is important to study the performance degradation for non-ideal case and also left as a future study.

References

[1] F. Adachi, M. Sawahashi, and H. Suda, "Wideband DS-CDMA for next generation mobile communications systems," IEEE Commun. Mag., vol.36, no.9, pp.56–69, Sept. 1998.
[2] R. Van Nee and R. Prasad, OFDM for wireless multimedia communications, Artech House, 2000.
[3] S. Hara and R. Prasad, "Overview of multicarrier CDMA," IEEE Commun. Mag., vol.35, no.12, pp.126–133, Dec. 1997.
[4] S. Hara and R. Prasad, Multicarrier techniques for 4G mobile communications, Artech House, 2003.
[5] S. Abeta, H. Atarashi, and M. Sawahashi, "Performance of coherent multi-carrier/DS-CDMA and MC-CDMA for broadband packet wireless access," IEICE Trans. Commun., vol.E84-B, no.3, pp.406–414, March 2001.
[6] F. Adachi, T. Sao, and T. Itagaki, "Performance of multicode DS-CDMA using frequency domain equalization in a frequency selective fading channel," Electron. Lett., vol.39, no.2, pp.239–241, Jan. 2003.
[7] T. Itagaki and F. Adachi, "Joint frequency domain equalization and antenna diversity combining for orthogonal multicode DS-CDMA signal transmissions in a frequency selective fading channel," IEICE Trans. Commun., vol.E87-B, no.7, pp.1954–1963, July 2004.
[8] F. Adachi and K. Takeda, "Bit error rate analysis of DS-CDMA with joint frequency-domain equalization and antenna diversity combining," IEICE Trans. Commun., vol.E87-B, no.10, pp.2991–3002, Oct. 2004.
[9] D. Garg and F. Adachi, "Throughput of RCPT hybrid ARQ for DS-CDMA with diversity reception and rake combining," Proc. IEEE VTC03 Spring, pp.2730–2734, Korea, April 2003.
[10] D. Garg and F. Adachi, "Rate compatible punctured turbo-coded hybrid ARQ for OFDM in a frequency selective fading channel," Proc. IEEE VTC03 Spring, pp.2725–2729, Korea, April 2003.
[11] A. Stefanov and T. Duman, "Turbo coded modulation for wireless communications with antenna diversity," Proc. IEEE VTC99-Fall, pp.1565–1569, Netherland, Sept. 1999.
[12] F. Adachi, K. Ohono, A. Higuchi, T. Dohi, and Y. Okumura, "Coherent multicode DS-CDMA mobile radio," IEICE Trans. Commun., vol.E79-B, no.9, pp.1316–1325, Sept. 1996.
[13] F. Adachi and T. Itagaki, "Frequency-domain rake combining for antenna diversity reception of DS-CDMA signals," IEICE Trans. Commun., vol.E86-B, no.9, pp.2781–2784, Sept. 2003.
[14] J. Hagenauer, "Rate-compatible punctured convolutional codes (RCPC codes) and their application," IEEE Trans. Commun., vol.36, no.4, pp.389–400, April 1988.
[15] F. Adachi, S. Ito, and K. Ohno, "Performance analysis of a time diversity ARQ in land mobile radio," IEEE Trans. Commun., vol.37, no.2, pp.177–183, Feb. 1989.
[16] F. Adachi and T. Sao, "Joint antenna diversity and frequency-domain equalization for multi-rate MC-CDMA," IEICE Trans. Commun., vol.E86-B, no.11, pp.3217–3224, Nov. 2003.
[17] J.P. Woodard and L. Hanzo, "Comparative study of turbo decoding techniques: An overview," IEEE Trans. Veh. Technol., vol.49, no.6, pp.2208–2233, Nov. 2000.
[18] C. Kchao and G.L. Stuber, "Analysis of a direct-sequence spread-spectrum cellular radio system," IEEE Trans. Commun., vol.41, no.10, pp.1507–1516, Oct. 1993.
[19] F. Adachi, "Transmit power efficiency of fast transmit power controlled DS-CDMA reverse link," IEICE Trans. Fundamentals, vol.E80-A, no.12, pp.2420–2428, Dec. 1997.
[20] P. Dent, G.E. Bottomley, and T. Croft, "Jakes fading model revisited," Electron. Lett., vol.29, no.13, pp.1162–1163, June 1993.
[21] 3GPP TR25.858, "Technical specification group radio access network; Physical layer aspects of UTRA high speed downlink packet access," version 4.0.0.
[22] K. Takeda, T. Itagaki, and F. Adachi, "Joint use of frequency-domain equalization and transmit/receive antenna diversity for single carrier transmissions," IEICE Trans. Commun., vol.E87-B, no.7, pp.1946–1953, July 2004.
[23] D. Garg and F. Adachi, "Performance comparison of turbo-coded DS-CDMA, MC-CDMA and OFDM with frequency-domain equalization and higher-level modulation," Proc. IEEE VTC04 Fall, USA, Sept. 2004.
[24] S. Lin and D.J. Costello, Error Control Coding: Fundamentals and Applications, Prentice Hall, 1983.

Appendix: Conditional Throughput Analysis for Uncoded ARQ

For parallel SW-ARQ as assumed in the paper, where the transmission channel can be fully utilized at all time, the throughput η is the same as for a selective-repeat ARQ and is given by [24]

$$\eta = (1 - \bar{P}). \tag{A·1}$$

where $\bar{P}$ is the average PER. The average PER can be found if the conditional PER P is known. The conditional PER for a given channel is computed from [24]

$$P = 1 - (1 - p_b\{H(k)\})^N \tag{A·2}$$

where $p_b\{H(k)\}$ is the conditional BER and N is the packet length in bits. In [8] the conditional BER is theoretically evaluated for MC-CDMA and DS-CDMA with MMSE-FDE when channel coding is not applied. It is shown that the conditional BER p_b is given by

$$p_b\{H(k)\} = \frac{1}{2} erfc\left[\sqrt{\frac{1}{4}\gamma\left(\frac{E_s}{N_0}, \{H(k)\}\right)}\right] \tag{A·3}$$

for QPSK, where

$$\gamma\left(\frac{E_s}{N_0}, \{H(k)\}\right) =$$

$$\begin{cases} \dfrac{\dfrac{2E_s}{N_0}\left|\dfrac{1}{N_c}\displaystyle\sum_{k=0}^{N_c-1}\tilde{H}(k)\right|^2}{\left[\begin{array}{l}\dfrac{1}{N_c}\displaystyle\sum_{k=0}^{N_c-1}|w(k)|^2 \\ +\left(\dfrac{C}{SF}\dfrac{E_s}{N_0}\right)\left\{\dfrac{1}{N_c}\displaystyle\sum_{k=0}^{N_c-1}|\tilde{H}(k)|^2-\left|\dfrac{1}{N_c}\displaystyle\sum_{k=0}^{N_c-1}\tilde{H}(k)\right|^2\right\}\end{array}\right]} \\ \text{for DS-CDMA} \\ \dfrac{\dfrac{2E_s}{N_0}\left|\dfrac{1}{SF}\displaystyle\sum_{k=0}^{SF_{MC}-1}\tilde{H}(k)\right|^2}{\left[\begin{array}{l}\dfrac{1}{SF}\displaystyle\sum_{k=0}^{SF-1}|w(k)|^2 \\ +\left(\dfrac{C-1}{SF}\dfrac{E_s}{N_0}\right)\left\{\dfrac{1}{SF}\displaystyle\sum_{k=0}^{SF-1}|\tilde{H}(k)|^2-\left|\dfrac{1}{SF}\displaystyle\sum_{k=0}^{SF-1}\tilde{H}(k)\right|^2\right\}\end{array}\right]} \\ \text{for MC-CDMA.} \end{cases} \tag{A$\cdot$4}$$

Calculating $p_b\{H(k)\}$ usings Eqs. (A· 3) and (A· 4), the conditional PER P for a given channel gains $\{H(k)\}$ can be obtained from Eq. (A· 2). Taking average of P for different set of channel gains $\{H(k)\}$, the throughput is obtained using Eq. (A· 1). For MC-CDMA and DS-CDMA with MMSE-FDE, the MMSE weight given in Eq. (4) is used. DS-CDMA with MRC-FDE is equivalent to rake combining in the time-domain [13]. Hence the numerical results for DS-CDMA with rake combing is found using the MRC weight shown in Eq. (8).

OFDM can be treated as a special case of MC-CDMA with SF=1. In OFDM, each subcarrier carries a different symbol. In a frequency selective channel, the statistics of the channel gain experienced by each subcarrier is equally likely for all subcarriers and the conditional packet error rate is given by

$$P = 1 - \prod_{k=0}^{N-1}(1 - p_b(H(k)). \tag{A$\cdot$5}$$

The average PER and hence the throughput can be obtained by averaging Eq. (A· 5) for different sets of channel gains $\{H(k)\}$.

Deepshikha Garg received her B.E. degree in Electrical and Communications engineering from Kathmandu University, Nepal in 1998. Currently she is in the Ph.D. program in the department of electrical and communications engineering at Tohoku University, Sendai, Japan. Her research interests include error control schemes and accessing techniques for wireless communications. She was the recipient of the 2002 active research award in radio communication systems from IEICE in 2002.

Fumiyuki Adachi received his B.S. and Dr. Eng. degrees in electrical engineering from Tohoku University, Sendai, Japan, in 1973 and 1984, respectively. In April 1973, he joined the Electrical Communications Laboratories of Nippon Telegraph & Telephone Corporation (now NTT) and conducted various types of research related to digital cellular mobile communications. From July 1992 to December 1999, he was with NTT Mobile Communications Network, Inc. (now NTT DoCoMo, Inc.), where he led a research group on wideband/broadband CDMA wireless access for IMT-2000 and beyond. Since January 2000, he has been with Tohoku University, Sendai, Japan, where he is a Professor of Electrical and Communication Engineering at Graduate School of Engineering. His research interests are in CDMA and TDMA wireless access techniques, CDMA spreading code design, Rake receiver, transmit/receive antenna diversity, adaptive antenna array, bandwidth-efficient digital modulation, and channel coding, with particular application to broadband wireless communications systems. From October 1984 to September 1985, he was a United Kingdom SERC Visiting Research Fellow in the Department of Electrical Engineering and Electronics at Liverpool University. From April 1997 to March 2000, he was a visiting Professor at Nara Institute of Science and Technology, Japan. He was a recipient of IEICE Achievement Award 2002 and was a co-recipient of the IEICE Transactions best paper of the year award 1996 and again 1998. He is an IEEE Fellow and was a co-recipient of the IEEE Vehicular Technology Transactions best paper of the year award 1980 and again 1990 and also a recipient of Avant Garde award 2000.